

A MODEL BASED SUPERVISION SYSTEM FOR THE HYDRAULICS OF PASSENGER CAR BRAKING SYSTEMS

Harald Straky, Marco Münchhof, Rolf Isermann

*Institute of Automatic Control
Laboratory of Control Engineering and Process Automation
Darmstadt University of Technology
Landgraf-Georg-Str. 4, D-64283 Darmstadt, Germany
Phone: +49 6151 16-7412, FAX: +49 6151 16-7421
{ hstraky, mmuenchhof, risermann}@iat.tu-darmstadt.de*

Abstract: This paper presents the design of a model-based supervision and diagnosis system for hydraulic and future electro-hydraulic passenger car braking systems. A state space model of the braking system has been derived, which allows calculation of the individual wheel brake cylinder pressures as well as the amount of brake fluid consumed due to faults in the braking system. Based on this model, a real-time supervision system has been developed, which allows early detection and diagnosis of leakages and air entrapments in the hydraulic subsystem. This supervision system only requires data of sensors which are already available in modern passenger cars.
Copyright © 2002 IFAC

Keywords: brakes, hydraulic, electro-hydraulic, fault detection, fault diagnosis

1. INTRODUCTION

The spatial (hardware-based) and functional (software-based) integration of control systems significantly improved the functionality of hydraulic braking systems (Fennel, 1998; Kiesewetter *et al.*, 1997; van Zanten *et al.*, 1998). Systems such as anti-lock braking (ABS), traction control (TCS), electronic stability program (ESP) or the brake assistant (BAS) transform the conventional hydraulic braking system into a complex mechatronic system, which actively supports the driver in critical situations, thus increasing active driving safety significantly. The anti-lock system supports the driver by controlling the wheel slip during braking maneuvers. A wheel lock up is prevented, ensuring that the car remains maneuverable even during difficult braking maneuvers. The traction control systems prevents wheel spin, which would cause a loss of traction and at the same time endanger vehicle stability. The electronic stability package supports the driver in critical lateral dynamic driving situations. A yawing torque is exerted by selectively braking individual wheels, thus keeping the vehicle on the desired path. The brake assistant supports the driver in emergency braking, by automatically applying the brakes fully, thus submitting all four wheels to ABS slip control.

The high level of control authority imparted to these security system necessitates permanent monitoring of all components. Measures currently implemented include active tests upon engine start and validity checks of sensor and actuator signals. Sensor faults and faults of the electronics such as short circuits and breaks can be detected reliably. Upon detection of a fault, the control system is shut down, leaving the driver with the conventional hydraulic braking system. Although the hydraulic system serves as a transmission path for all control commands issued by the control systems and although the braking system is the last back-up level, it is the only subsystem that is not monitored in current designs. The only security measure is a redundant design which divides the braking system into two separate circuits. If one braking circuit drops out, the other circuit still remains functional providing 50% of the normal braking power. This causes an elongation in the braking distance and can give rise to unexpected lateral behavior. Research carried out at the University of Technology at Darmstadt has shown that influences of braking system faults on vehicle dynamics cannot be compensated by the average driver (Straky *et al.*, 2001). Even small faults can have severe consequences: For example, spraying brake fluid can drench the brake disk, drastically reducing friction and thus the force that can be generated by the brake.

These issues show that early detection of small faults of the hydraulic system is of major importance.

The main causes of brake system failures are leakages, air and water entrancements. Water inclusions are harmful because of vaporization. Most defects are due to wearout (e.g. porous or cut-through hoses), incorrect maintenance (e.g. air entrancements) or neglected maintenance (e.g. water inclusions).

The paper will describe the design of a fault detection and diagnosis system for hydraulic braking systems. First, a model of the hydraulic braking system is derived. In the following, this model will be used to generate reference values for the amount of brake fluid consumed by the braking system. The model will be fed by pressure sensors mounted at the master brake cylinder. The effective amount of fluid consumed is determined from the vacuum brake booster diaphragm displacement. Thus, one can obtain two different values for the volume consumed by the braking system. The difference between these two volumes indicates the presence and the severity of a fault. In addition to this information, the system is also able to distinguish between air inclusions and leakages. A correlation analysis based technique is used for the fault classification. Numerical examples prove the feasibility of the chosen approach, the fidelity of the brake system model and the accuracy of the fault detection and classification methods.

2. THEORETICAL MODEL

In this section, a model of the braking system will be derived. The internal dynamics of the ABS/ESP system are not taken into account. For the hydraulic unit, only those control valves are modeled, which are open during normal driving operation. Normal operation will refer to the ABS having no control authority over the pressure buildup. A schematic view of the simplified hydraulic circuit is presented in Fig. 1.

The mechanical design already offers a certain degree of fault tolerance, because the hydraulic system has been divided into two brake circuits, each acting on two of the four wheel brakes. Two diagonally opposing brake cylinders are interconnected inside the hydraulic unit, thus forming one brake circuit. Each circuit is supplied with fluid from one chamber of the master brake cylinder. The intermediate piston, located inside the master brake cylinder, seals the two circuits. If a pressure loss occurs in brake circuit I, the left return spring is compressed fully and the intermediate piston abuts the housing, thereby enabling a pressure buildup in circuit II. On the contrary, if a pressure loss disables brake circuit II, the push-rod piston will come into contact with the intermediate piston as the right return spring gives way. This allows pressurization of circuit I. In both cases, the available braking force is halved by the loss of

one circuit, whereas the operating force that the driver must apply remains unchanged.

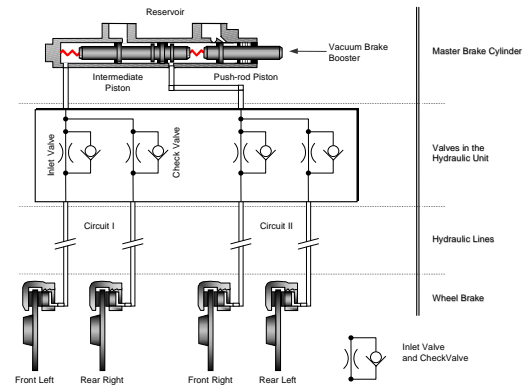


Fig. 1: Schematic View of the Hydraulic System

Central valves are built into the master brake cylinder allowing equalization of the fluid level due to changes in the temperature or due to worn brake pads. If the brakes are released, the two central valves open and brake fluid can be exchanged with the fluid reservoir via the sniffer holes.

Hydraulic lines conjoin the master brake cylinder and the hydraulic unit. Valves in the hydraulic unit can direct the hydraulic flow in different ways. As was already mentioned, the hydraulic unit will be modeled as being inactive. In this mode, the inlet valves are open. In parallel to each inlet valve, there is a check valve, whose task is to expedite releasing the brakes. Four brake lines transport the brake fluid to the wheel brake cylinders. This is where the piston presses the friction pads against the brake disks. In conjunction with the floating caliper, the pressure dependent clamping forces are generated. More detailed descriptions of hydraulic and electrohydraulic brake systems for passenger cars can be found in (Burckhardt, 1991) and (ITT Automotive, 1995).

The hydraulic system will be modeled as a process with lumped parameters. Employing the analogy between electric and hydraulic circuits (Isermann, 1999; Backe, 1992), the brake system can be described by four four-terminal electric networks (one per wheel brake). In this model, both brake circuits are decoupled, as can be seen in Fig. 2. The pedal force exerted by the driver pressurizes the chambers of the master brake cylinder. Pressure corresponds to voltage in the electric equivalent circuit diagram. Thus, the pressure signals from the sensors are modeled as ideal voltage sources. A capacitance is connected in parallel to each voltage source capturing the compressibility of the fluid enclosed in the master brake cylinder.

Upon pressurization of the master brake cylinder chambers, brake fluid will be forced into the wheel

brake cylinders. The flow to the individual wheels is denoted as \dot{V}_{fl} , \dot{V}_{fr} , \dot{V}_{rl} , and \dot{V}_{rr} .

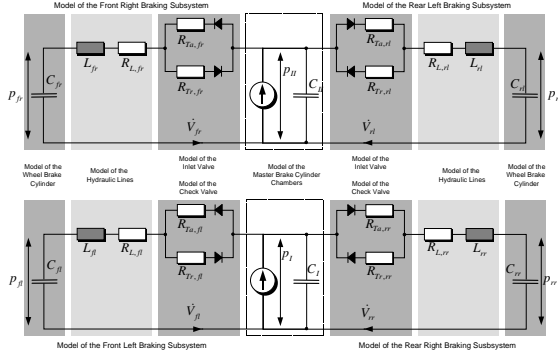


Fig. 2: Equivalent Circuit Diagram of the Hydraulic Braking System

The inlet valves located inside the hydraulic unit drastically reduce the stream area in comparison to the conduits. Therefore, these constrictions represent large hydraulic resistances. Using Bernoulli's equation, the valves in the hydraulic unit have been modeled as orifices assuming turbulent flow through the valve mouth. The loss coefficient depends on the direction of the flow due to the aforementioned check valves. In the equivalent circuit diagram, the dependency on flow direction has been taken into account by the inclusion of two diodes and two resistors, $R_{Ta,i}$ and $R_{Tr,i}$, $i \in \{fl, fr, rl, rr\}$, per valve combination.

The inertia of mass of the fluid contained in the conduits antagonizes any change of velocity. This effect is captured by four inductances L_i . The subsystems, which embody the transmission line characteristics, also contain linear resistors, which replicate the laminar flow losses in the tubes.

The four wheel brake cylinders have been modeled as non-linear capacitances $C_i(V_i)$, which capture the non-linear $p_i - V_i$ characteristics of the individual brakes. These curves are illustrated in Fig. 3. The running of these curves is influenced by the compressibility of the fluid contained in the brake lines, the pressure-induced hose widening, the broadening of the caliper and the air gap between the friction pads and the brake disk, which must be traversed by the friction pads if the brakes are engaged.

The condensed state space representation of the entire braking system is given as

$$\begin{aligned} \dot{\underline{x}} &= \underline{a}(\underline{x}) + \underline{B} \cdot \underline{u} \\ y &= \underline{c}^T \cdot \underline{x} + \underline{d}^T \cdot \underline{u} \end{aligned} \quad (1)$$

with the state vector

$$\underline{x} = (V_{fl} \ \dot{V}_{fl} \ V_{fr} \ \dot{V}_{fr} \ V_{rl} \ \dot{V}_{rl} \ V_{rr} \ \dot{V}_{rr})^T \quad (2)$$

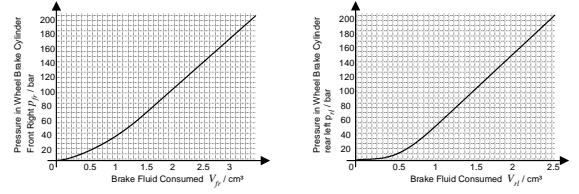


Fig. 3: Nonlinear Relation between Pressure Applied at and Volume ingested by the Wheel Brake Cylinder.

Left: Front Right Wheel Brake Cylinder
Right: Rear Left Wheel Brake Cylinder

and the state space matrix

$$\underline{a}(\underline{x}) = \begin{pmatrix} \dot{V}_{fl} \\ -\frac{R_{T,fl}}{L_{fl}} \cdot \dot{V}_{fl}^2 - \frac{R_{L,fl}}{L_{fl}} \cdot \dot{V}_{fl} - \frac{1}{L_{fl}} \cdot \int \frac{\dot{V}_{fl}}{C_{fl}(V_{fl})} dt \\ \dot{V}_{fr} \\ -\frac{R_{T,fr}}{L_{fr}} \cdot \dot{V}_{fr}^2 - \frac{R_{L,fr}}{L_{fr}} \cdot \dot{V}_{fr} - \frac{1}{L_{fr}} \cdot \int \frac{\dot{V}_{fr}}{C_{fr}(V_{fr})} dt \\ \dot{V}_{rl} \\ -\frac{R_{T,rl}}{L_{rl}} \cdot \dot{V}_{rl}^2 - \frac{R_{L,rl}}{L_{rl}} \cdot \dot{V}_{rl} - \frac{1}{L_{rl}} \cdot \int \frac{\dot{V}_{rl}}{C_{rl}(V_{rl})} dt \\ \dot{V}_{rr} \\ -\frac{R_{T,rr}}{L_{rr}} \cdot \dot{V}_{rr}^2 - \frac{R_{L,rr}}{L_{rr}} \cdot \dot{V}_{rr} - \frac{1}{L_{rr}} \cdot \int \frac{\dot{V}_{rr}}{C_{rr}(V_{rr})} dt \end{pmatrix} \quad (3)$$

The input distribution matrix

$$\underline{B} = \begin{pmatrix} 0 & 0 & 0 & \frac{1}{L_{fr}} & 0 & \frac{1}{L_{rl}} & 0 & 0 \\ 0 & \frac{1}{L_{fl}} & 0 & 0 & 0 & 0 & 0 & \frac{1}{L_{rr}} \end{pmatrix}^T \quad (4)$$

is allocating the input vector

$$\underline{u} = \begin{pmatrix} p_{fl} \\ p_{rl} \end{pmatrix}. \quad (5)$$

These two master brake cylinder chamber pressures are recorded by pressure sensors in current production passenger cars. The model output, i.e. the amount of brake fluid consumed, is determined by the output distribution vector

$$\underline{c}^T = (1 \ 0 \ 1 \ 0 \ 1 \ 0 \ 1 \ 0) \quad (6)$$

and the direct transmission vector

$$\underline{d}^T = (C_{fl} \ C_{rl}). \quad (7)$$

The turbulent resistance is piecewise constant, assuming the values

$$R_{T,i} = \begin{cases} R_{Ta,i} & \text{for } \dot{V}_i \geq 0 \\ R_{Tr,i} & \text{for } \dot{V}_i < 0 \end{cases} \quad (8)$$

The integrals in the \underline{a} matrix evaluate to

$$\int \frac{\dot{V}_i}{C_i(V_i)} dt = p_i(V_i), \quad i \in \{fl, fr, rl, rr\} \quad (9)$$

All system parameters have been identified by analysis of experimental data. These data have been obtained from measurements at a test-bed as described in (Straky *et al.*, 2001)

3. MODEL VALIDATION

Although the amount of liquid consumed by the braking system cannot be measured, it is still possible to validate the model. Validation can be carried out by comparing the wheel brake pressure sensor signals with the reconstructed wheel brake pressure, exploiting equation (9). Figure 4 shows a comparison between simulation and experimental data for the front left and rear left wheel. These diagrams not only prove the high fidelity of the model, they also illustrate the difference in dynamics.

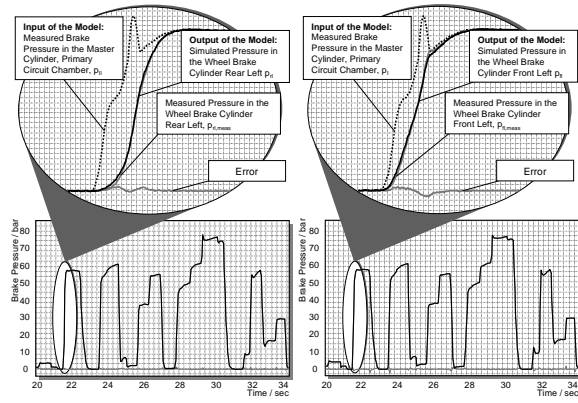


Fig 4: Comparison of Simulation and Measurements
Left: Rear Left Wheel Brake Cylinder
Right: Front Left Wheel Brake Cylinder

4. MODEL BASED FAULT DETECTION

The state space system described in the preceding section allows the calculation of the amount of hydraulic fluid consumed by a fault-free braking system. This information does not suffice to implement fault-detection methods since no direct measurement of the effective amount of consumed brake fluid is available. This information must thus be reconstructed.

The displacement of the push-rod piston correlates to the amount of fluid pumped into the braking system. Unfortunately, sensory information about the actual location of the push-rod piston is not available. However, looking at the cut-away drawing of the vacuum brake booster in Fig. 5, one can see that the reaction washer couples the push-rod piston and the diaphragm. The diaphragm position is already sensed in modern passenger cars. This information can be transformed using the diaphragm displacement-volume consumed relation shown in Fig. 5. The non-linearity is introduced by the compressibility of the reaction washer which is made out of rubber.

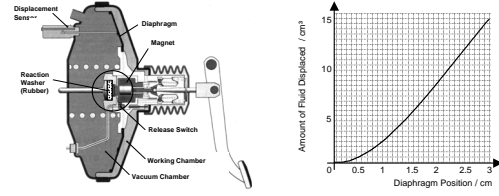


Fig. 5: Influence of the Reaction Washer on the Calculation of the Volume Consumed by the Braking System

Once the effective volume has been obtained, one can look at the difference between the reference volume V_{Ref} and the actual volume V_{Act} consumed by the brake system. The difference of these two volumes yields V_{Fault} , i.e. the change in the consumed volume due to faults. A value close to zero signals fault-free operation, meaning that there are no air entrapments, no leakages and no unusual hose widenings.

5. FAULT MODELING AND DIAGNOSIS

The aforementioned calculation of V_{Fault} provides direct information about the severity of a fault. The type of fault, i. e. leakage, air inclusion and so forth, can be determined by employing a correlation analysis approach.

The correlation coefficient provides a measure for the degree of linear dependency between two signals $x(t)$ and $y(t)$. The magnitude of the correlation coefficient ρ is constrained by $|\rho| \leq 1$, where a value close to either -1 or +1 signals a linear relation between the two signals. The correlation coefficient for two discrete signals (Papoulis, 1991) is given by

$$\rho_{xy} = \frac{\eta_{xy} - \eta_x \eta_y}{\sigma_x \sigma_y}, \quad (10)$$

where the mean values are given as

$$\eta_{xy} = \frac{1}{N} \left(\sum_{i=1}^N x(i) \cdot y(i) \right) \quad (11)$$

$$\eta_x = \frac{1}{N} \left(\sum_{i=1}^N x(i) \right) \quad (12)$$

$$\eta_y = \frac{1}{N} \left(\sum_{i=1}^N y(i) \right) \quad (13)$$

and the standard deviations are

$$\sigma_x = \sqrt{\frac{1}{N} \left(\sum_{i=1}^N x^2(i) \right) - \frac{1}{N} \left(\sum_{i=1}^N x(i) \right)^2} \quad (14)$$

and

$$\sigma_y = \sqrt{\frac{1}{N} \left(\sum_{i=1}^N y^2(i) \right) - \frac{1}{N} \left(\sum_{i=1}^N y(i) \right)^2} \quad (15)$$

by definition. N denotes the number of samples. Since the algorithm will be employed for on-line

fault detection and diagnosis, a slightly different calculation scheme has been implemented. The significance of the correlation coefficient increases with the number of data points. The main advantage of the correlation analysis over other methods is the fast and easy calculation, which is essential for the performance of a real-time capable fault-detection and diagnosis system.

In order to classify the fault occurred, the procedure needs information about the behavior of V_{Fault} in the presence of different types of system errors. Therefore, models of typical brake system faults will now be derived.

Leakages can be modeled as orifices. The volume flowing through such openings is given by

$$V_{Fault}(t) = k_{Leak} \cdot \int \sqrt{|p_{Leak}(t) - p_{Amb}(t)|} dt \quad (16)$$

where k_{Leak} is the unknown leakage coefficient and p_{Leak} is the fluid pressure at the damaged spot. This pressure itself is not known but can be approximated by the master brake cylinder pressure, thus

$$V_{Fault}(t) \sim \int \sqrt{|p_{Leak}(t) - p_{Amb}(t)|} dt \sim \int \sqrt{|p_I(t) - p_{Amb}(t)|} dt \quad (17)$$

p_{Amb} denotes the atmospheric pressure. Thus, if the loss volume V_{Fault} correlates with the integral of the square root of the excess pressure in one of the main brake chambers, this would allude to the presence of a leakage.

If air is entrapped in the braking system, this air will be compressed upon pressurization of the braking system. Isothermal compression and expansion have been assumed. The equation of states for ideal gasses yields

$$V_{Air}(t) \cdot p_{Air}(t) = V_{Air,Amb} \cdot p_{Amb}, \quad (18)$$

where V_{Air} denotes the volume of the air entrapment subject to the pressure p_{Air} . $V_{Air,Amb}$ denotes the initial volume at atmospheric pressure p_{Amb} . Upon pressurization, the air inclusions give way, resulting in more fluid being drained from the master brake cylinder. This additional volume is given as

$$V_{Fault}(t) = V_{Air,Amb} - V_{Air}(t) = V_{Air,Amb} \cdot \frac{p_{Air}(t) - p_{Amb}}{p_{Air}(t)} \quad (19)$$

The actual pressure in the air entrapments is unknown and also approximated by the pressure in the master brake cylinder, leading to

$$V_{Fault}(t) \sim \frac{p_I(t) - p_{Amb}}{p_I(t)} \quad (20)$$

Based on this derivation, the fault diagnosis system will analyze the correlation coefficients

$$V_{Fault} \cdot \frac{p_I - p_{Amb}}{p_I} \Rightarrow \rho_{Air} \quad (21)$$

$$V_{Fault} \cdot \int \sqrt{|p_I - p_{Amb}|} \Rightarrow \rho_{Leak}$$

The first correlation coefficient, ρ_{Air} , signals air inclusions, whereas the latter, ρ_{Leak} , reacts on leakages. Figure 6 shows the structure of the model based fault detection and diagnosis system, which has been developed in this paper.

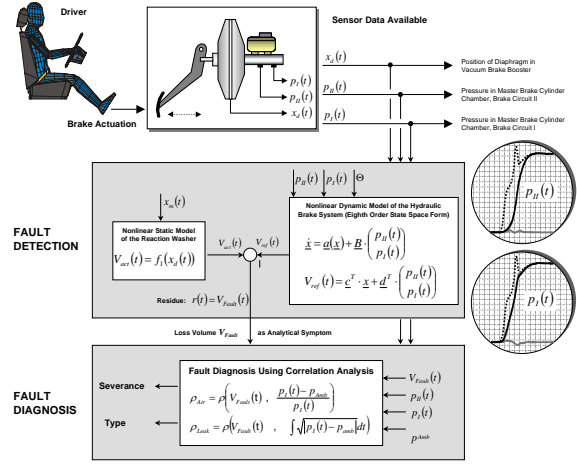


Fig. 6: Structure of the Model Based Fault Detection and Diagnosis System

6. RESULTS

In this section, the performance of the fault detection and diagnosis algorithm is evaluated. Figure 7 shows a series of brake actuations. The first segment depicts the fault-free case, whereas the other three segments illustrate the behavior in the presence of faults. The experimental setup has allowed the inclusion of two kinds of faults, namely air entrapments and leakages.

To summarize the findings, faulty behavior has always been detected very early and reliably. Upon detection of a fault, on-line calculation of the correlation coefficients will be initiated. Figure 7 displays the development of both correlation coefficients and the volume V_{Fault} over time.

As was already stated, the first case illustrates the fault free case. For the second brake actuation, the correlation coefficient ρ_{Air} is larger than ρ_{Leak} . The diagnosis system will thus conclude that there is air entrapped in the system.

The next segment illustrates the effects of including a leakage. Now, the correlation coefficient ρ_{Leak} is much larger than ρ_{Air} , which diminishes over time. The fault diagnosis system would consequently report a leakage to the driver.

For the fourth and last brake operation, the correlation coefficient ρ_{Leak} runs back to zero after its initial jump to +1. The other correlation coefficient goes to -1 and remains there. Recalling that values of both +1 and -1 indicate correlation, the fault would correctly be classified as an air entrapment.

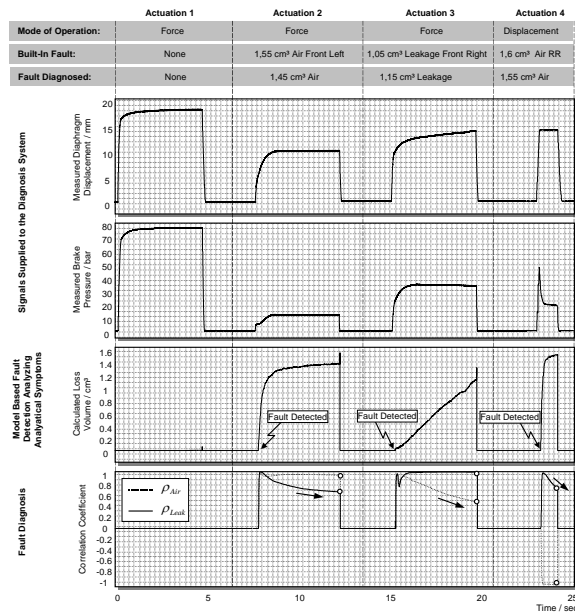


Fig. 7: On-line Fault Detection and Diagnosis

7. CONCLUSIONS

This paper discussed the design of a model-based fault detection and diagnosis system. It was illustrated how the functional integration of analytical process knowledge can expand the functionality of a mechatronic system by providing the driver with information about the state of the braking system and by warning him of arising errors, which might eventually lead to accidents.

First, a model of the hydraulic braking system was derived. This development was based on the analogy between hydraulic and electric circuits and resulted in an eighth order non-linear system. All parameters have been identified from measurements at a braking system test-bed. Comparisons of simulations and experimental data have proven the high fidelity of the model.

Based on this model, a fault detection and diagnosis system has been implemented, which allows early detection, diagnosis and localization of small, drifting faults such as leakages or air entrapments in the hydraulic system. This fault detection and diagnosis procedure supervises the amount of brake fluid consumed by the brake system. The reference value is generated by utilizing the aforementioned brake system model, which is fed by pressure sensors mounted at the master brake cylinder chambers. The

effective amount of fluid consumed is calculated from the displacement of the vacuum brake booster diaphragm.

Two common types of faults are classified, air inclusions and leakages. Classification is accomplished by employing a correlation analysis scheme. The main advantage of this method is the small computational expense resulting in real-time capability of the algorithm.

The supervision system only requires data of sensors which are already available in modern passenger cars. Due to the likeness of hydraulic and electro-hydraulic braking systems, it is easily possible to use the presented methods to cover electro-hydraulic braking systems as well. Here, one can use more affluent sensor signals, since all four wheel brake pressures and the pressure and volume stored in the accumulator are sensed. These additional information allow wheel-individual fault detection and diagnosis.

Upon detection, diagnosis and localization of faults, the system can initiate countermeasures such as for example inform the driver about necessary maintenance or repair work. This paper contributes enormously to an increase in driving safety of passenger cars.

REFERENCES

- Backé, W. (1992): *Grundlagen der Ölhydraulik*, Vorlesungsumdruck der RWTH - Aachen
- Burckhardt, M. (1991): *Bremsdynamik und Pkw-Bremsanlagen*, Reihe Fahrwerktechnik, Vogel Fachbuch.
- Fennel, H. (1998): Ein Konzept zur Beherrschung der Fahrdynamik, *Automobiltechnische Zeitschrift ATZ 100*, 302 ff.
- Isermann, R. (1999): *Mechatronische Systeme*, Springer Verlag.
- ITT-Automotive (1995): *Bremsen Handbuch - Elektronische Bremsysteme*, Autohaus-Verlag.
- Kiesewetter W., Klinkner W., Reichelt W., Steiner M. (1997): Der neue Brake-Assist von Mercedes-Benz, *Automobiltechnische Zeitschrift ATZ 99*, S. 330 ff.
- Papoulis, A. (1991): *Probability, Random Variables and Stochastic Processes* 3rd Edition, Boston WCB/McGraw-Hill.
- Straky, H., Kochem, M., Schmitt, J., Hild, R., Isermann, R. (2001). Influences of Braking System Faults on the Vehicle Dynamics. *3rd IFAC Workshop Advances in Automotive Control*, 28th-30th March 2001, Karlsruhe, Germany.
- van Zanten A., Erhardt R., Landesfeind K., Pfaff G. (1998): VDC System Development, *International Congress & Exposition SAE*, 23-26 February, Detroit.